



# High frequency repetitive transcranial magnetic stimulation to the left dorsolateral prefrontal cortex modulates sensorimotor cortex function in the transition to sustained muscle pain

Enrico De Martino<sup>a</sup>, David A. Seminowicz<sup>a,c,d</sup>, Siobhan M. Schabrun<sup>b</sup>, Laura Petrini<sup>a</sup>, Thomas Graven-Nielsen<sup>a,\*</sup>

<sup>a</sup> Center for Neuroplasticity and Pain (CNAP), SMI, Department of Health Science and Technology, The Faculty of Medicine, Aalborg University, Denmark

<sup>b</sup> Brain Rehabilitation and Neuroplasticity Unit (BRAiN-u), Western Sydney University, School of Science and Health, Sydney, Australia

<sup>c</sup> Department of Neural and Pain Sciences, University of Maryland School of Dentistry, Baltimore, MD, 21201, USA

<sup>d</sup> Center to Advance Chronic Pain Research, University of Maryland Baltimore, Baltimore, MD, 21201, USA

## ARTICLE INFO

### Keywords:

Persistent muscle hyperalgesia  
Neuroplasticity  
Repetitive transcranial magnetic stimulation  
Dorsolateral prefrontal cortex  
Cortical excitability

## ABSTRACT

Based on reciprocal connections between the dorsolateral prefrontal cortex (DLPFC) and basal-ganglia regions associated with sensorimotor cortical excitability, it was hypothesized that repetitive transcranial magnetic stimulation (rTMS) of the left DLPFC would modulate sensorimotor cortical excitability induced by muscle pain. Muscle pain was provoked by injections of nerve growth factor (end of Day-0 and Day-2) into the right extensor carpi radialis brevis (ECRB) muscle in two groups of 15 healthy participants receiving 5 daily sessions (Day-0 to Day-4) of active or sham rTMS. Muscle pain scores and pressure pain thresholds (PPTs) were collected (Day-0, Day-3, Day-5). Assessment of motor cortical excitability using TMS (mapping cortical ECRB muscle representation) and somatosensory evoked potentials (SEPs) from electrical stimulation of the right radial nerve were recorded at Day-0 and Day-5. At Day-0 versus Day-5, the sham compared to active group showed: Higher muscle pain scores and reduced PPTs ( $P < 0.04$ ); decreased frontal N30 SEP ( $P < 0.01$ ); increased TMS map volume ( $P < 0.03$ ). These results indicate that muscle pain exerts modulatory effects on the sensorimotor cortical excitability and left DLPFC rTMS has analgesic effects and modulates pain-induced sensorimotor cortical adaptations. These findings suggest an important role of prefrontal to basal-ganglia function in sensorimotor cortical excitability and pain processing.

## 1. Introduction

Chronic musculoskeletal pain is the leading cause of disability worldwide and maladaptive neuroplastic mechanisms play a crucial role in the transition from acute to chronic pain (Kuner and Flor, 2016). For this reason, interventions able to reverse or, perhaps most importantly, to prevent pain neuroplasticity may be pivotal in the future management of musculoskeletal pain.

In recent years several different neurophysiological measurements have been applied to investigate cortical neuroplasticity during pain with heterogeneous findings (Chang et al., 2018), probably due to the fact that they target different neurobiological structures. Within these

neurophysiological measurements, motor evoked potentials (MEPs) and somatosensory evoked potentials (SEPs) have been frequently used to explore cortical neuroplasticity since they are generated in specific sensorimotor cortical areas. For instance, using transcranial magnetic stimulation (TMS), increase excitability of the primary motor cortex (M1) have been repeatedly demonstrated after motor learning (Pascual-Leone et al., 1994a,b). Similarly, using electrical stimulation of a nerve, neuroplastic changes in primary sensory cortex (S1) have been observed after transient anesthetic de-afferentation (Tinazzi et al., 1997). Based on sensory and motor evoked potentials, cortical neuroplasticity has been documented in patients affected by chronic musculoskeletal pain and in healthy subjects using different experimental pain models (Flor et al.,

\* Corresponding author. Center for Neuroplasticity and Pain (CNAP), SMI, Department of Health Science and Technology, Faculty of Medicine, Aalborg University, Fredrik Bajers Vej 7D-3, 9220, Aalborg E, Denmark.

E-mail address: [tgn@hst.aau.dk](mailto:tgn@hst.aau.dk) (T. Graven-Nielsen).

URL: <http://www.cnap.hst.aau.dk/~tgn> (T. Graven-Nielsen).

<https://doi.org/10.1016/j.neuroimage.2018.10.076>

Received 20 July 2018; Received in revised form 8 October 2018; Accepted 29 October 2018

Available online 1 November 2018

1053-8119/© 2018 Elsevier Inc. All rights reserved.

1997; Le Pera et al., 2001; Rossi et al., 2003; Tsao et al., 2008), indicating that nociceptive inputs induce neuroplastic changes in motor and sensory cortical excitability.

Applying repetitive TMS (rTMS) to cortical areas, temporary changes in cortical excitability have been described (Ziemann et al., 2008), offering the unique opportunity to non-invasively target the neural excitability of specific cortical and subcortical areas during pain (Kobayashi and Pascual-Leone, 2003). Lasting beneficial effects have been seen in about 40% of patients with medication-resistant depression after multiple sessions. Promising results have also been described in chronic neuropathic pain, motor strokes and Parkinson's (Lefaucheur et al., 2014).

Depending on several parameters, such as stimulation frequency, target, number of pulses, coil orientation (Rossini et al., 2015), rTMS can exert facilitatory or inhibitory effects on the stimulated cortex in healthy subjects. For instance, low-frequency rTMS (1 Hz) to M1 has been demonstrated to generally induce a lasting decrease in motor cortical excitability (Chen et al., 1997), while high-frequency stimulation has been observed to generally increase excitability of the motor cortex (Pascual-Leone et al., 1994).

The dorsolateral prefrontal cortex (DLPFC) is a functionally and structurally heterogeneous region of the brain implicated in emotion, cognition and behavior (Glasser et al., 2016). Recent evidence has also shown that DLPFC plays a key role in pain suppression and detection (Seminowicz and Moayedi, 2017). For instance, using neuroimaging techniques, nociceptive stimuli in healthy subjects have shown a response of the left DLPFC (Freund et al., 2009). In addition, rTMS to the left DLPFC has been applied as a therapeutic target in short-lasting experimentally induced pain (Ciampi De Andrade et al., 2014; Taylor et al., 2012), as well as post-surgical pain (Borckardt et al., 2008, 2014), indicating that left DLPFC rTMS has a modulatory effects on pain detection. In addition, left DLPFC has several reciprocal connections with brain regions associated with sensorimotor cortical excitability, including the caudate nucleus, putamen, substantia nigra, and the thalamus (Alexander, 1986; Aron et al., 2007; Chudler and Dong, 1995; Middleton, 2002), making it reasonable to propose that left DLPFC stimulation modulates the sensorimotor cortical excitability through its effects on subcortical regions (Fierro et al., 2010).

In addition, when multiple sessions are applied that rTMS effect outlasts the stimulation period, in particular, as has been demonstrated in patients affected by chronic pain (Lefaucheur et al., 2014). However, the effect of multiple sessions of rTMS on nociceptive pain has not been tested and it is unknown whether the multiple sessions of rTMS to left DLPFC on musculoskeletal pain has analgesic and neuromodulatory effects.

Prolonged muscle pain and soreness induced by intramuscular injections of nerve growth factor (NGF) has recently been described as a model to provoke muscle soreness over several days (Bergin et al., 2015) with a reversible increase of the cortical M1 excitability of the painful muscle (De Martino et al., 2018; Schabrun et al., 2016), and altered frontal and parietal cortical somatosensory excitability (De Martino et al., 2018), providing the unique opportunity to test whether rTMS to left DLPFC modulates an early phase of cortical pain-evoked neuroplasticity.

The present study aimed to investigate the effect of multiple sessions of rTMS over the left DLPFC on sensorimotor cortical excitability in response to prolonged muscle soreness. It was hypothesized that pain and sensorimotor cortical changes (motor and sensory evoked potentials) evoked by a standardized model of muscle soreness (induced by injections of NGF) would be modulated by high frequency rTMS to left DLPFC.

## 2. Material and methods

### 2.1. Subjects

Thirty healthy right-handed subjects (18 females) participated in this

randomized controlled study. All participants were naïve to TMS prior to enrolment, and without any history of chronic musculoskeletal pain, neurological disorders or psychiatric disorders. Fifteen participants were randomly assigned to each of the active or sham high frequency rTMS groups (9 females for each group). The age, height, and weight (mean  $\pm$  standard error of the mean) for the sham and active groups, respectively, were  $26 \pm 1.4$  years and  $26.9 \pm 1.0$  years,  $172.2 \pm 2.9$  cm and  $170.2 \pm 2.2$  cm, and  $75 \pm 4.7$  kg and  $69.3 \pm 3.5$  kg. A TMS safety screen was completed before starting experimental procedures (Rossi et al., 2012). The study was approved by the local Ethics Committee (N-20170041) and was performed in accordance with the Helsinki Declaration. Other findings of this protocol are published elsewhere and include effects of rTMS on pain, muscle soreness, disability, painful area, and cognitive task performance (Seminowicz et al., 2018).

### 2.2. Study protocol

The study comprised 6 sessions on 6 consecutive days (Day-0 to Day-5). Muscle soreness was induced and maintained by injections of NGF (end of sessions at Day-0 and Day-2) into the right extensor carpi radialis brevis (ECRB) muscle in both groups (active, sham). Each session at Day-0, Day-3, and Day-5 began with administration of pain related questionnaires. After this, at Day-0 and Day-5, motor and sensory cortical excitability was assessed by TMS to map the cortical muscle representation of ECRB and by somatosensory evoked potentials (SEPs) evoked from electrical stimulation of the right radial nerve. Pain sensitivity measures and muscle strength were collected at Day-0, Day-3, and Day-5 (after SEP and TMS). Finally, participants received five daily sessions (Day-0 to Day-4) of active (N = 15) or sham (N = 15) rTMS. Participants were naïve to the rTMS procedure and not informed about the group allocation.

### 2.3. NGF-induced muscle soreness

Muscle pain was induced by injections of Beta-NGF into the ECRB muscle (Bergin et al., 2015). Sterile solutions of recombinant human Beta-NGF were prepared by the pharmacy (Skanderborg Apotek, Denmark). After cleaning the skin with alcohol, the injection (5  $\mu$ g/0.5 mL; 1-mL syringe with a disposable needle (27G)) into the muscle belly of ECRB was guided in-plane under real-time ultrasound guidance (De Martino et al., 2018).

### 2.4. Pain related questionnaires

Muscle soreness was assessed on a 7-point Likert scale where 0: represented 'a complete absence of pain/soreness'; 1: 'a light pain/soreness in the muscle felt only when touched/a vague ache'; 2: 'a moderate pain/soreness felt only when touched/a slight persistent ache'; 3: 'a light muscle pain/soreness when lifting objects or carrying objects'; 4: 'a light muscle pain/soreness, stiffness or weakness when moving the wrist or elbow without gripping an object'; 5: 'a moderate muscle pain/soreness, stiffness or weakness when moving the wrist or elbow'; and 6: 'a severe muscle pain/soreness, stiffness or weakness that limits my ability to move' (Bergin et al., 2015).

The patient rated tennis elbow evaluation (PRTEE) questionnaire was used to assess average disability of the right arm referring to the 24 h period prior data collection. Total score ranging from 0 (no pain and no functional impairment) to 100 (worst pain imaginable with significant functional impairment) (MacDermid, 2005).

Finally, participants drew the distribution of muscle soreness on an anatomical drawing of the upper limb. The areas of the body chart drawings were calculated in arbitrary units (a.u.) using a scanning program (VistaMetrix, v.1.38.0).

## 2.5. Motor evoked potentials and motor map

Single-pulse transcranial magnetic stimulation (TMS) was delivered (Magstim, 2002<sup>2</sup>; Magstim Co. Ltd) using a figure-of-eight shaped coil (D70<sup>2</sup> Coil, Magstim Co. Ltd). Participants were seated and maintained their hand and forearm relaxed with the wrist pronated throughout the experiment. With a swimming cap marked with a 1 × 1 cm stimulation grid and orientated to the vertex of the head, the coil was located over the left hemisphere at a 45-degree angle to the sagittal plane to induce current in a posterior-to-anterior direction (Schabrun et al., 2016). Using surface disposable silver/silver chloride adhesive recording electrodes (Ambu Neuroline 720) bipolar mounted in parallel with the muscle fibre, MEPs were recorded over the right ECRB muscle. The reference electrode was located on the right olecranon. MEP signals were band-pass filtered at 5 Hz - 1 kHz, sampled at 2 kHz, and digitized by a 16-bit data-acquisition card (National Instruments, NI6122).

The optimal cortical site (hotspot) of the right ECRB muscle was determined as the coil position that evoked a maximal peak-to-peak MEP for a given stimulation intensity. At the beginning of each session on Day-0 and Day-5, two measures were collected at the hotspot: 1) Resting motor threshold (rMT), defined as the minimum stimulation intensity at which 5 out of 10 stimuli applied at the hotspot evoked a response with a peak-to-peak amplitude of a minimum 50 μV (Schabrun et al., 2016). 2) Based on the MEPs of 10 stimuli at 120% of rMT at the hotspot site, the peak-to-peak amplitudes were extracted and averaged for analysis (Schabrun et al., 2016).

Using a TMS intensity of 120% rMT, the motor cortical map was established based on MEPs evoked every 6 s with a total of 5 stimuli at each site on the stimulation grid (Schabrun et al., 2016; De Martino et al., 2018). All grid sites were pseudo randomly stimulated from the hotspot until no MEP was recorded (defined as <50 μV peak-to-peak amplitude) in all five stimuli at all border sites (Schabrun et al., 2016). The number of active map sites (map area) and map volume were calculated off-line. If the average peak-to-peak amplitude of the 5 MEPs evoked at that site was greater than 50 μV, the site was considered ‘active’ (Schabrun and Ridding, 2007). The averaged peak-to-peak MEP amplitudes at all active sites were summed to calculate the map volume. The center of gravity (CoG) was defined as the amplitude-weighted center of the map (Wassermann et al., 1992) and was calculated by  $\frac{\sum V_i \cdot X_i}{\sum V_i}$ ;  $\frac{\sum V_i \cdot Y_i}{\sum V_i}$ ; where  $V_i$  represents mean MEP amplitude at each site with the coordinates  $X_i$ ,  $Y_i$  (Uy et al., 2002). For each session, the average peak-to-peak MEP amplitude at all sites across subjects were linearly interpolated to generate the MEP maps used for illustration of group effects.

## 2.6. Somatosensory evoked potentials

The right radial nerve was stimulated (1 ms duration at a rate of 2 Hz, 3 times the perceptual threshold) at the wrist with a bipolar electrode (Model 895340, Axelgaard, Fallbrook, cathode placed on the right radial styloid process and the anode two cm proximal) via an electrically isolated stimulator (NoxiTest IES 230). This intensity was considered comfortable by all participants.

An electrode cap including 64 electrodes was used (g.GAMMA cap<sup>2</sup>) where the F3, F1, Fc3, Fc1, C3, C1, Cp3, Cp1, P3 and P1 scalp sites were collected and referenced to the right earlobe (Oostenveld and Praamstra, 2001). The cap was mounted according to 10-5 system with Cz orientated to the vertex of the head. An additional electrooculographic electrode (Fp1) was recorded superior to the left eye to monitor eye-related movements. The ground electrode in the cap was placed half way between the eyebrows. Electrode impedances were kept below 5 kΩ. Electroencephalographic signals were amplified (50000x) and sampled at 2400 Hz (g.HIamp biosignal amplifier).

Two blocks of 500 stimuli were collected for all trials, filtered off-line at 5–500 Hz and contaminated traces were rejected before analysis (blinks, eye movements, or contraction of scalp musculature). The

artefact-free waveforms were averaged and the peaks P14, N18, P20, N30, P45 and N60 in the frontal leads and P14, N20, P25, N33, P45 and N60 in the parietal traces (Desmedt and Cheron, 1980) were identified, normalized to the pre-stimulation interval (subtracting the mean amplitude in the interval from –100 ms to –20 ms before the electrical stimulation) and the amplitudes and latencies were extracted.

## 2.7. Pressure pain sensitivity

Pressure pain thresholds (PPTs) were recorded using a handheld pressure algometer (1-cm<sup>2</sup> probe, Algometer type II, SBMEDIC Electronics) at each of 4 sites: Bilateral ECRB muscle, and bilateral tibialis anterior (TA) muscle (Bergin et al., 2015). The PPT was defined as the pressure intensity where the perception of pressure changed to a perception of pain. The average PPT of the 3 measures at each site was used for analysis.

## 2.8. Wrist extension force

Participants were seated with their right elbow positioned in pronation and 90° flexion. Isometric wrist extension force was recorded via a force sensor (MC3A 250, AMTI) mounted above the hand. Three maximal voluntary contractions (MVC) were performed to record the force exerted during the wrist extension contractions (Mista et al., 2016). The maximal wrist extension force among the three trials was used for analysis.

## 2.9. Repetitive active and sham transcranial magnetic stimulation

Repetitive TMS was delivered (Magstim Super Rapid<sup>2</sup> Plus<sup>1</sup>, Magstim Co. Ltd) to the left DLPFC using a figure-of-eight shaped coil (70 mm, Double Air Film Coil) oriented at a tangent to the scalp, with the main phase of the induced current in the anterior-posterior direction. The rTMS protocol consisted of one session per day for 5 consecutive days (Day-0 to Day-4). Each stimulation session consisted of 80 trains of 5 s pulses with a frequency of 10 Hz and an interval of 10 s between each train, giving a total of 4000 pulses per session (Taylor et al., 2012). The stimulation intensity was 110% of the rMT of the first dorsal interosseous muscle detected by visual inspection and the coil was located at the left DLPFC according to the BeamF3 algorithm (Beam et al., 2009; Mir-Moghtadaei et al., 2016). Sham stimulation was carried out with a sham coil of identical size, color, and shape, emitting a sound similar to that emitted by the active coil (70 mm Double Air Film Sham Coil). The participants were fitted with earplugs during rTMS and they rated the potential pain of the rTMS stimulation on an 11-point numerical rating scale (0: ‘no pain’, 10: ‘most intense pain imaginable’) (Borckardt et al., 2013). Potential side effects of rTMS (e.g. headache, nausea, mood changes) were carefully recorded.

## 2.10. Statistics

All data are presented as mean and standard error of the mean (SEM). Statistical significance was set at  $P < 0.05$ . To test for normality, all data were assessed using Shapiro-Wilk normality test. A mixed model analysis of variance (ANOVA) was used to assess within-subject effects of Day, between-subject effects of Group, and Day-by-Group interaction. Where appropriate, post-hoc analyses were performed using Bonferroni-corrected multiple comparison tests. To compensate for the use of multiple ANOVAs in the analysis of EEG data (10 recording sites) the P-value from the ANOVAs was Bonferroni corrected to  $P < 0.005$  (i.e. 0.05/10) for accepting significant factors or interactions. Spearman correlation analyses were performed between the differences relative to Day-0 of pain related questionnaires (Likert scale and PRTEE) and pressure pain sensitivity, respectively, and neurophysiological outcomes at Day-5. Only significant changes over Day and Group in neurophysiological outcomes were considered for correlation. Significance of multiple correlation analyses were Bonferroni corrected. Finally, the association between

procedural pain and muscle soreness scores was tested using Pearson correlations.

### 3. Results

#### 3.1. Experimental muscle soreness

The Likert scores of muscle soreness on Day-3 and Day-5 were higher in the sham rTMS group than the active rTMS group (Table 1; ANOVA:  $F_{1,28} = 17.68$ ;  $P < 0.001$ ). Likewise, on Day-3 and Day-5 the PRTEE were higher in the sham rTMS group compared with the active rTMS group (ANOVA:  $F_{1,28} = 4.83$ ;  $P = 0.036$ ). The perceived muscle soreness was distributed mainly along the radial side of the forearm (Fig. 1) and the area (Day-3 and Day-5) was larger in the sham than active rTMS group (ANOVA:  $F_{1,28} = 11.93$ ;  $P = 0.002$ ).

#### 3.2. Pressure pain sensitivity

The ANOVA of PPTs measured over the right ECRB muscle revealed a Day-by-Group interaction (Table 1; ANOVA:  $F_{2,56} = 3.69$ ;  $P = 0.047$ ). At Day-3 and Day-5, post-hoc analysis showed that the PPT on the right ECRB muscle was lower in the sham group compared with the active rTMS group ( $P < 0.039$ ) and reduced in both groups compared with Day-0 ( $P < 0.001$ ). The ANOVA of PPTs measured over the left ECRB muscle revealed a main effect of Day (ANOVA:  $F_{2,56} = 5.21$ ,  $P = 0.015$ ). Compared with Day-0, PPTs were reduced at the left ECRB muscle at Day-5 ( $P = 0.043$ ). No difference in the PPT was found over the right or left TA muscle (Day-by-Group ANOVA interaction:  $F_{2,56} < 0.91$ ;  $P > 0.46$ ).

#### 3.3. Wrist extension force

The ANOVA of maximal wrist extension force for the right hand showed a main effect of Day (Table 1; ANOVA:  $F_{2,56} = 6.56$ ,  $P = 0.003$ ). Compared with Day-0 the maximum force was reduced at Day-3 and Day-5 ( $P < 0.038$ ).

#### 3.4. Sensory evoked potentials

Fig. 2 shows the 10 recording sites, located in the contralateral hemisphere to the right radial nerve stimulation. A widely distributed positive far-field P14 potentials was presented in all recording electrodes (Desmedt and Cheron, 1980; Mauguière et al., 1983) (e.g. F1 and P1), followed by the subcortical frontal N18 potential (Desmedt and Cheron,

**Table 1**

Mean ( $\pm$ SEM,  $N = 15$ ) parameters related with the experimental muscle pain model. Likert scale scores, PRTEE (patient rated tennis elbow evaluation), Area of pain, pressure pain threshold (PPT) on left and right ECRB and TA muscles and right max wrist force are illustrated for the sham and active rTMS groups. Significant post-hoc tests from Day-0 within the group (\*,  $P < 0.05$ ) and between groups within the day (#,  $P < 0.05$ ).

	Group	Day-0	Day-3	Day-5
Likert scores (0–6)	Sham	–	4.4 $\pm$ 0.2#	4.2 $\pm$ 0.2#
	Active	–	3.4 $\pm$ 0.3#	2.6 $\pm$ 0.3#
PRTEE (0–100)	Sham	–	29.3 $\pm$ 4.2#	23.2 $\pm$ 3.7#
	Active	–	21.9 $\pm$ 4.5#	13.2 $\pm$ 2.8#
Area of pain (a.u.)	Sham	–	16.38 $\pm$ 1.4#	12.5 $\pm$ 1.2#
	Active	–	10.75 $\pm$ 1.3#	7.26 $\pm$ 0.9#
PPT left ECRB (kPa)	Sham	214.7 $\pm$ 17.2	198.8 $\pm$ 20.6	183.8 $\pm$ 20.8*
	Active	239.0 $\pm$ 28.7	220.8 $\pm$ 28.8	215.6 $\pm$ 22.6*
PPT right ECRB (kPa)	Sham	238.4 $\pm$ 24.4	108.3 $\pm$ 12.9*#	111.0 $\pm$ 15.6*#
	Active	245.7 $\pm$ 27.9	151.1 $\pm$ 73.7*#	152.7 $\pm$ 20.9*#
PPT left TA (kPa)	Sham	375.8 $\pm$ 45.8	372.4 $\pm$ 59.1	377.9 $\pm$ 50.3
	Active	438.5 $\pm$ 58.3	437.1 $\pm$ 61.3	453.7 $\pm$ 64.4
PPT right TA (kPa)	Sham	437.6 $\pm$ 46.2	438.4 $\pm$ 55.5	434.2 $\pm$ 60.3
	Active	489.5 $\pm$ 70.1	495.5 $\pm$ 69.4	488.1 $\pm$ 64.0
Max force (N)	Sham	144.9 $\pm$ 12.9	135.5 $\pm$ 11.8*	132.6 $\pm$ 11.0*
	Active	163.0 $\pm$ 18.5	156.7 $\pm$ 18.2*	154.0 $\pm$ 17.9*

1980) (F1). The N20 potential (P1), representing the earliest cortical response, was identified in the lateral parietal region followed by the P25 positivity and N33 negativity (Allison et al., 1989) (Cp1). Differently, the frontal P20 positivity was followed by a large frontal N30 negativity (Cebolla et al., 2011) (Fc1). Finally, a widely distributed P45 potential could be recognized in all traces, followed by a diffuse N60 potential (Valeriani et al., 2001) (C1).

Significant Day-by-Group interaction was found for the N30 amplitude in the F1 and Fc1 recording sites (Fig. 2, Table 2, and Supplement Material 1). At Day-5, compared with Day-0, the peak amplitude of N30 on F1 and Fc1 recording sites decreased in the sham group ( $P < 0.001$ ). On the F1 recording site of the active rTMS group, the N30 peak amplitude increased at Day-5 compared with Day-1 ( $P = 0.04$ ), whereas on the Fc1 recording site the amplitude tended to increase ( $P = 0.06$ ). At Day-5 the N30 peak amplitude on F1 and Fc1 were higher in the active compared with the sham rTMS group ( $P < 0.01$ ). On Cp1 recording sites (Fig. 2), the peak amplitude of N33 increased at Day-5 compared with Day-0 in both groups (Table 2 and Supplement Material 2).

On F3, F1, Fc3, Fc1, C3, C1, and Cp1 recording sites (Fig. 2), the P45 peak amplitude increased at Day-5 compared with Day-0 in both the sham and active rTMS groups (Table 2 and Supplement Material 3).

For all recording sites, the peak amplitudes of P14 (Day\*Group ANOVA:  $F_{1,28} < 1.19$ ,  $P > 0.28$ ), N20 (Day\*Group ANOVA:  $F_{1,28} < 9.28$ ,  $P > 0.005$ ), P20/P25 (Day\*Group ANOVA:  $F_{1,28} < 3.77$ ,  $P > 0.06$ ) and N60 (Day\*Group ANOVA:  $F_{1,28} < 1.47$ ,  $P > 0.23$ ) were not significantly altered over Groups and Days. There were no latency changes for any of the peaks under investigation (data not presented).

#### 3.5. Motor evoked potentials

The MEP area and volume was increased at Day-5 compared with Day-0 in the sham group and reduced at Day-5 compared with Day-0 in the active rTMS group (Fig. 3). Significant Day-by-Group interaction was found for the MEP map volume, number of active sites (map area), rest motor threshold (rMT), and MEP amplitude in the hot spot (Table 3). At Day-5 compared with Day-0, post-hoc analysis showed increased map volume and number of active sites in the sham group ( $P < 0.001$ ) whereas the active rTMS group showed decreased map volume ( $P = 0.001$ ) and no significant difference in the number of active sites ( $P = 0.17$ ). At Day-5, map volume and the number of active sites were lower in the active rTMS group compared with the sham group ( $P < 0.03$ ). The ANOVA of CoG positions were not significantly affected over Day and Group (Table 3).

#### 3.6. Sensory and motor evoked potentials correlated with hyperalgesia and muscle soreness

Likert scale, PRTEE, PPT on ECRB muscle, N30 SEPs amplitude on F1 recording site, and MEP map volume were considered for correlations. Compared to Day-0, Day-5 showed an increase in muscle soreness scores (Likert scale) which was associated with decrease in N30 amplitude at F1 recording sites (i.e. change scores in muscle soreness correlated with change scores in N30; Fig. 4A; Spearman  $R = -0.58$ ,  $P = 0.01$ ). A reduction in PPTs (hyperalgesia) in the right ECRB muscle was also associated with the decrease of N30 amplitude (Fig. 4B; Spearman  $R = 0.53$ ,  $P = 0.04$ ). Furthermore, the increase of MEP map volume were associated with the decrease of N30 amplitude (Fig. 4C; Spearman  $R = -0.54$ ,  $P = 0.03$ ). Finally, Pearson correlations did not reveal significant association between procedural pain and muscle soreness soreness the subsequent day (data not reported).

#### 3.7. Side effects related to rTMS

No unexpected side effects were observed during and after the intervention. Consistent with previous reports (Borckardt et al., 2006), the rTMS protocol itself produced pain. The procedural pain rating

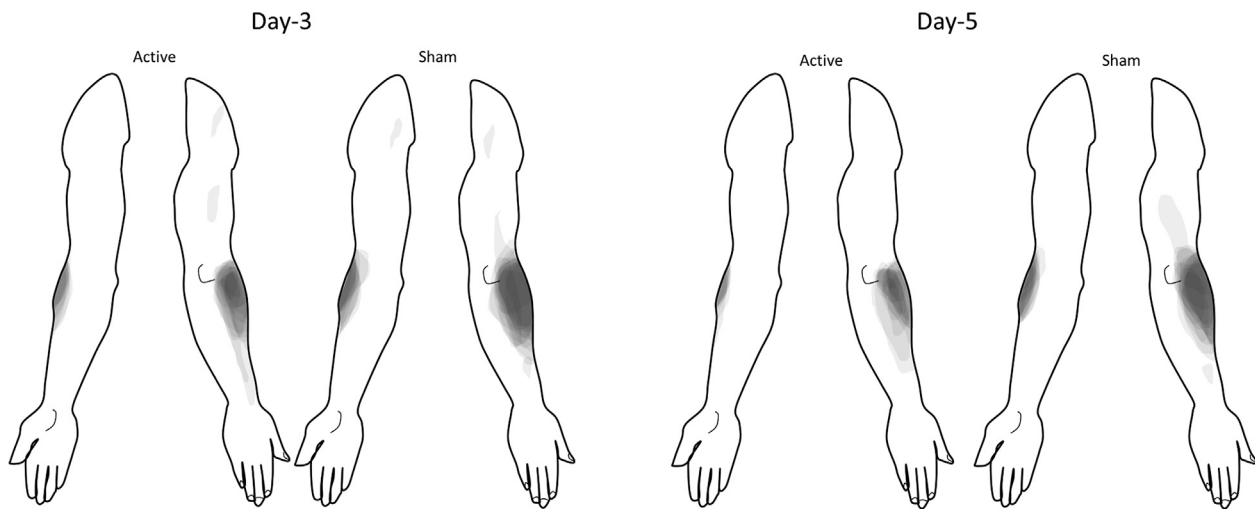


**Fig. 1.** Body chart pain drawings (anterior and posterior view of the right arm) showing distribution of muscle pain at Day-3 and Day-5 following injection of nerve growth factor into the extensor carpi radialis brevis muscle (Day-0 and Day-2) in the groups receiving active ( $N = 15$ ) and sham ( $N = 15$ ) rTMS applied daily at Day-0 to Day-4.

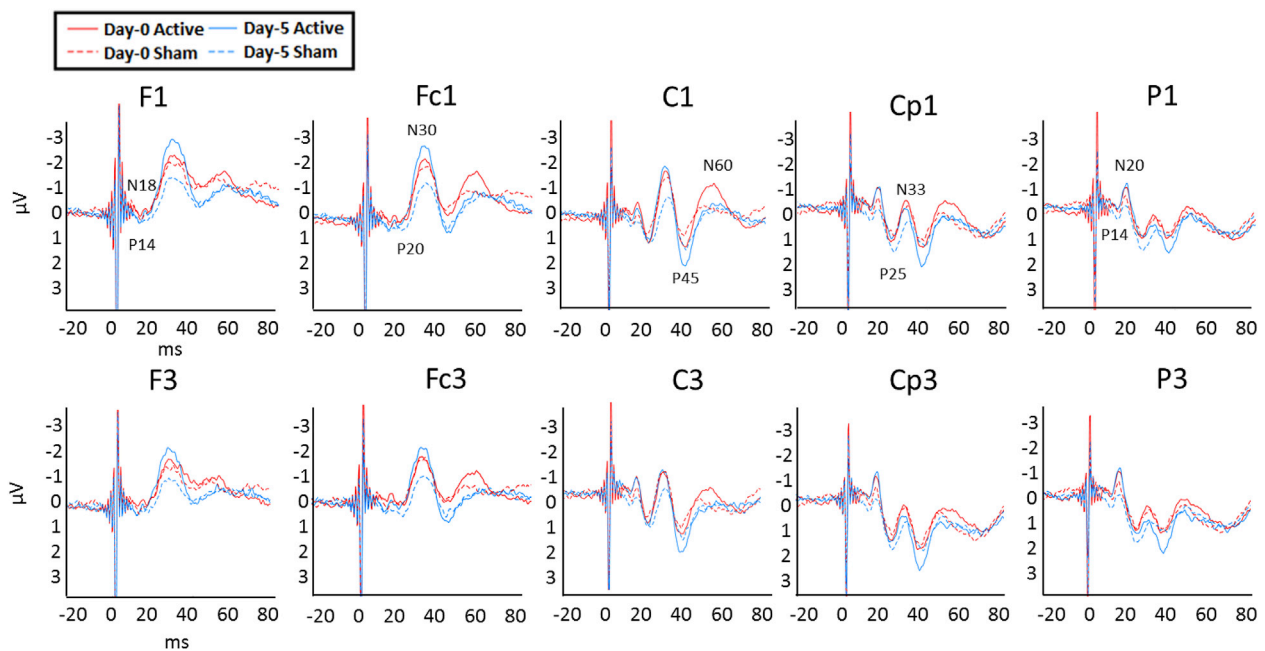


**Fig. 2.** Grand average ( $N = 15$ ) of SEPs from right radial nerve stimulation recorded by frontal electrodes (F3, F1, Fc3, Fc1) and central-parietal electrodes (C3, C1, Cp3, Cp1, P3 and P1) scalp sites placed according to the 10–20 system. Traces from Day-0 (red lines) and Day-5 (blue lines) are illustrated after nerve growth factor injections into the extensor carpi radialis brevis muscle in the group receiving active (solid lines) and sham (broken lines) rTMS applied daily at Day-0 to Day-5.

reduced across days from the first (Day-0) to the fifth session (Day-4) in the active rTMS group from  $5.6 \pm 0.8$  in the first session to  $2.9 \pm 0.6$  in the last session. No subjects reported any pain immediately after the intervention or one day after the last intervention (Day-4). No pain was reported by the sham group.

#### 4. Discussion

The present study examined the cortical neuroplastic consequences after multiple sessions of high frequency rTMS applied to left DLPFC while experimental muscle soreness developed over several days in otherwise healthy participants. The results suggest that left DLPFC rTMS, which reduced muscle soreness, functional disability and muscle hyperalgesia relative to sham, modulated the sensorimotor cortical changes

(motor and sensory evoked potentials) induced by muscle pain. More specifically, in the sham rTMS group, experimental muscle soreness was associated with increased motor cortex excitability and decreased frontal sensory-evoked excitability, whereas the opposite changes were seen in the active rTMS group.

##### 4.1. Effects of left DLPFC rTMS on experimental muscle pain

The results of the present study showed that multiple days stimulations of left DLPFC stimulation can reduce the muscle soreness, disability in hand function and muscle hyperalgesia associated with long-lasting experimental muscle pain. Similar to previous studies and in the sham group, injections of NGF into the ECRB muscle evoked moderate muscle soreness (Likert scale:  $\sim 4$  (Bergin et al., 2015; Schabrun et al., 2016),)

**Table 2**

Mean ( $\pm$ SEM, N = 15) sensory evoked potential (SEP) component for each peak electrode. F-values and P-values (significance accepted at 0.005 due to multiple ANOVAs) are from the mixed-model ANOVA. Significant post-hoc tests from Day-0 within the group (\*,  $P < 0.05$ ) and between groups within the day (#,  $P < 0.05$ ).

SEP Component	Peak electrode	Group	Day-0	Day-5	Mixed model repeated-measures ANOVA																																																																																					
					Day	Group	Day*Group																																																																																			
P14	F1	Sham	0.51 $\pm$ 0.10	0.64 $\pm$ 0.12	$F_{1,28} = 2.83$ , $P = 0.103$	$F_{1,28} = 0.43$ , $P = 0.517$	$F_{1,28} = 0.10$ , $P = 0.754$																																																																																			
		Active	0.40 $\pm$ 0.10	0.48 $\pm$ 0.17				N18	Fc3	Sham	-0.14 $\pm$ 0.09	-0.04 $\pm$ 0.11	$F_{1,28} = 6.13$ , $P = 0.019$	$F_{1,28} = 3.75$ , $P = 0.060$	$F_{1,28} = 0.33$ , $P = 0.568$	Active	-0.43 $\pm$ 0.13	-0.23 $\pm$ 0.15	N20	Cp1	Sham	-0.58 $\pm$ 0.11	-0.24 $\pm$ 0.11	$F_{1,28} = 3.07$ , $P = 0.090$	$F_{1,28} = 6.58$ , $P = 0.016$	$F_{1,28} = 4.13$ , $P = 0.051$	Active	-0.81 $\pm$ 0.17	-0.94 $\pm$ 0.15	P20	Fc3	Sham	0.53 $\pm$ 0.13	0.78 $\pm$ 0.14	$F_{1,28} = 2.81$ , $P = 0.104$	$F_{1,28} = 0.11$ , $P = 0.746$	$F_{1,28} = 0.41$ , $P = 0.528$	Active	0.52 $\pm$ 0.21	0.50 $\pm$ 0.24	P25	Cp1	Sham	1.33 $\pm$ 0.20	1.68 $\pm$ 0.24	$F_{1,28} = 2.02$ , $P = 0.166$	$F_{1,28} = 0.15$ , $P = 0.697$	$F_{1,28} = 3.47$ , $P = 0.06$	Active	1.51 $\pm$ 0.30	1.54 $\pm$ 0.34	N30	F1	Sham	-1.64 $\pm$ 0.24	-1.20 $\pm$ 0.23*#	$F_{1,28} = 0.10$ , $P = 0.750$	$F_{1,28} = 4.25$ , $P = 0.048$	$F_{1,28} = 11.3$ , $P = 0.002$	Active	-1.86 $\pm$ 0.24	-2.24 $\pm$ 0.26*#	N33	Cp1	Sham	-0.59 $\pm$ 0.21	-0.11 $\pm$ 0.17*	$F_{1,28} = 10.3$ , $P = 0.003$	$F_{1,28} = 0.29$ , $P = 0.592$	$F_{1,28} = 1.00$ , $P = 0.326$	Active	-0.60 $\pm$ 0.20	-0.35 $\pm$ 0.23*	P45	Cp1	Sham	1.35 $\pm$ 0.16	1.59 $\pm$ 0.22*	$F_{1,28} = 9.8$ , $P = 0.004$	$F_{1,28} = 1.2$ , $P = 0.276$	$F_{1,28} = 2.1$ , $P = 0.161$	Active	1.45 $\pm$ 0.26	2.10 $\pm$ 0.30*	N60	Fc1	Sham	-1.44 $\pm$ 0.75	-1.27 $\pm$ 0.24	$F_{1,28} = 1.57$ , $P = 0.219$
N18	Fc3	Sham	-0.14 $\pm$ 0.09	-0.04 $\pm$ 0.11	$F_{1,28} = 6.13$ , $P = 0.019$	$F_{1,28} = 3.75$ , $P = 0.060$	$F_{1,28} = 0.33$ , $P = 0.568$																																																																																			
		Active	-0.43 $\pm$ 0.13	-0.23 $\pm$ 0.15				N20	Cp1	Sham	-0.58 $\pm$ 0.11	-0.24 $\pm$ 0.11	$F_{1,28} = 3.07$ , $P = 0.090$	$F_{1,28} = 6.58$ , $P = 0.016$	$F_{1,28} = 4.13$ , $P = 0.051$	Active	-0.81 $\pm$ 0.17	-0.94 $\pm$ 0.15	P20	Fc3	Sham	0.53 $\pm$ 0.13	0.78 $\pm$ 0.14	$F_{1,28} = 2.81$ , $P = 0.104$	$F_{1,28} = 0.11$ , $P = 0.746$	$F_{1,28} = 0.41$ , $P = 0.528$	Active	0.52 $\pm$ 0.21	0.50 $\pm$ 0.24	P25	Cp1	Sham	1.33 $\pm$ 0.20	1.68 $\pm$ 0.24	$F_{1,28} = 2.02$ , $P = 0.166$	$F_{1,28} = 0.15$ , $P = 0.697$	$F_{1,28} = 3.47$ , $P = 0.06$	Active	1.51 $\pm$ 0.30	1.54 $\pm$ 0.34	N30	F1	Sham	-1.64 $\pm$ 0.24	-1.20 $\pm$ 0.23*#	$F_{1,28} = 0.10$ , $P = 0.750$	$F_{1,28} = 4.25$ , $P = 0.048$	$F_{1,28} = 11.3$ , $P = 0.002$	Active	-1.86 $\pm$ 0.24	-2.24 $\pm$ 0.26*#	N33	Cp1	Sham	-0.59 $\pm$ 0.21	-0.11 $\pm$ 0.17*	$F_{1,28} = 10.3$ , $P = 0.003$	$F_{1,28} = 0.29$ , $P = 0.592$	$F_{1,28} = 1.00$ , $P = 0.326$	Active	-0.60 $\pm$ 0.20	-0.35 $\pm$ 0.23*	P45	Cp1	Sham	1.35 $\pm$ 0.16	1.59 $\pm$ 0.22*	$F_{1,28} = 9.8$ , $P = 0.004$	$F_{1,28} = 1.2$ , $P = 0.276$	$F_{1,28} = 2.1$ , $P = 0.161$	Active	1.45 $\pm$ 0.26	2.10 $\pm$ 0.30*	N60	Fc1	Sham	-1.44 $\pm$ 0.75	-1.27 $\pm$ 0.24	$F_{1,28} = 1.57$ , $P = 0.219$	$F_{1,28} = 0.72$ , $P = 0.403$	$F_{1,28} = 0.00$ , $P = 0.989$	Active	-1.70 $\pm$ 0.25	-1.56 $\pm$ 0.33						
N20	Cp1	Sham	-0.58 $\pm$ 0.11	-0.24 $\pm$ 0.11	$F_{1,28} = 3.07$ , $P = 0.090$	$F_{1,28} = 6.58$ , $P = 0.016$	$F_{1,28} = 4.13$ , $P = 0.051$																																																																																			
		Active	-0.81 $\pm$ 0.17	-0.94 $\pm$ 0.15				P20	Fc3	Sham	0.53 $\pm$ 0.13	0.78 $\pm$ 0.14	$F_{1,28} = 2.81$ , $P = 0.104$	$F_{1,28} = 0.11$ , $P = 0.746$	$F_{1,28} = 0.41$ , $P = 0.528$	Active	0.52 $\pm$ 0.21	0.50 $\pm$ 0.24	P25	Cp1	Sham	1.33 $\pm$ 0.20	1.68 $\pm$ 0.24	$F_{1,28} = 2.02$ , $P = 0.166$	$F_{1,28} = 0.15$ , $P = 0.697$	$F_{1,28} = 3.47$ , $P = 0.06$	Active	1.51 $\pm$ 0.30	1.54 $\pm$ 0.34	N30	F1	Sham	-1.64 $\pm$ 0.24	-1.20 $\pm$ 0.23*#	$F_{1,28} = 0.10$ , $P = 0.750$	$F_{1,28} = 4.25$ , $P = 0.048$	$F_{1,28} = 11.3$ , $P = 0.002$	Active	-1.86 $\pm$ 0.24	-2.24 $\pm$ 0.26*#	N33	Cp1	Sham	-0.59 $\pm$ 0.21	-0.11 $\pm$ 0.17*	$F_{1,28} = 10.3$ , $P = 0.003$	$F_{1,28} = 0.29$ , $P = 0.592$	$F_{1,28} = 1.00$ , $P = 0.326$	Active	-0.60 $\pm$ 0.20	-0.35 $\pm$ 0.23*	P45	Cp1	Sham	1.35 $\pm$ 0.16	1.59 $\pm$ 0.22*	$F_{1,28} = 9.8$ , $P = 0.004$	$F_{1,28} = 1.2$ , $P = 0.276$	$F_{1,28} = 2.1$ , $P = 0.161$	Active	1.45 $\pm$ 0.26	2.10 $\pm$ 0.30*	N60	Fc1	Sham	-1.44 $\pm$ 0.75	-1.27 $\pm$ 0.24	$F_{1,28} = 1.57$ , $P = 0.219$	$F_{1,28} = 0.72$ , $P = 0.403$	$F_{1,28} = 0.00$ , $P = 0.989$	Active	-1.70 $\pm$ 0.25	-1.56 $\pm$ 0.33																	
P20	Fc3	Sham	0.53 $\pm$ 0.13	0.78 $\pm$ 0.14	$F_{1,28} = 2.81$ , $P = 0.104$	$F_{1,28} = 0.11$ , $P = 0.746$	$F_{1,28} = 0.41$ , $P = 0.528$																																																																																			
		Active	0.52 $\pm$ 0.21	0.50 $\pm$ 0.24				P25	Cp1	Sham	1.33 $\pm$ 0.20	1.68 $\pm$ 0.24	$F_{1,28} = 2.02$ , $P = 0.166$	$F_{1,28} = 0.15$ , $P = 0.697$	$F_{1,28} = 3.47$ , $P = 0.06$	Active	1.51 $\pm$ 0.30	1.54 $\pm$ 0.34	N30	F1	Sham	-1.64 $\pm$ 0.24	-1.20 $\pm$ 0.23*#	$F_{1,28} = 0.10$ , $P = 0.750$	$F_{1,28} = 4.25$ , $P = 0.048$	$F_{1,28} = 11.3$ , $P = 0.002$	Active	-1.86 $\pm$ 0.24	-2.24 $\pm$ 0.26*#	N33	Cp1	Sham	-0.59 $\pm$ 0.21	-0.11 $\pm$ 0.17*	$F_{1,28} = 10.3$ , $P = 0.003$	$F_{1,28} = 0.29$ , $P = 0.592$	$F_{1,28} = 1.00$ , $P = 0.326$	Active	-0.60 $\pm$ 0.20	-0.35 $\pm$ 0.23*	P45	Cp1	Sham	1.35 $\pm$ 0.16	1.59 $\pm$ 0.22*	$F_{1,28} = 9.8$ , $P = 0.004$	$F_{1,28} = 1.2$ , $P = 0.276$	$F_{1,28} = 2.1$ , $P = 0.161$	Active	1.45 $\pm$ 0.26	2.10 $\pm$ 0.30*	N60	Fc1	Sham	-1.44 $\pm$ 0.75	-1.27 $\pm$ 0.24	$F_{1,28} = 1.57$ , $P = 0.219$	$F_{1,28} = 0.72$ , $P = 0.403$	$F_{1,28} = 0.00$ , $P = 0.989$	Active	-1.70 $\pm$ 0.25	-1.56 $\pm$ 0.33																												
P25	Cp1	Sham	1.33 $\pm$ 0.20	1.68 $\pm$ 0.24	$F_{1,28} = 2.02$ , $P = 0.166$	$F_{1,28} = 0.15$ , $P = 0.697$	$F_{1,28} = 3.47$ , $P = 0.06$																																																																																			
		Active	1.51 $\pm$ 0.30	1.54 $\pm$ 0.34				N30	F1	Sham	-1.64 $\pm$ 0.24	-1.20 $\pm$ 0.23*#	$F_{1,28} = 0.10$ , $P = 0.750$	$F_{1,28} = 4.25$ , $P = 0.048$	$F_{1,28} = 11.3$ , $P = 0.002$	Active	-1.86 $\pm$ 0.24	-2.24 $\pm$ 0.26*#	N33	Cp1	Sham	-0.59 $\pm$ 0.21	-0.11 $\pm$ 0.17*	$F_{1,28} = 10.3$ , $P = 0.003$	$F_{1,28} = 0.29$ , $P = 0.592$	$F_{1,28} = 1.00$ , $P = 0.326$	Active	-0.60 $\pm$ 0.20	-0.35 $\pm$ 0.23*	P45	Cp1	Sham	1.35 $\pm$ 0.16	1.59 $\pm$ 0.22*	$F_{1,28} = 9.8$ , $P = 0.004$	$F_{1,28} = 1.2$ , $P = 0.276$	$F_{1,28} = 2.1$ , $P = 0.161$	Active	1.45 $\pm$ 0.26	2.10 $\pm$ 0.30*	N60	Fc1	Sham	-1.44 $\pm$ 0.75	-1.27 $\pm$ 0.24	$F_{1,28} = 1.57$ , $P = 0.219$	$F_{1,28} = 0.72$ , $P = 0.403$	$F_{1,28} = 0.00$ , $P = 0.989$	Active	-1.70 $\pm$ 0.25	-1.56 $\pm$ 0.33																																							
N30	F1	Sham	-1.64 $\pm$ 0.24	-1.20 $\pm$ 0.23*#	$F_{1,28} = 0.10$ , $P = 0.750$	$F_{1,28} = 4.25$ , $P = 0.048$	$F_{1,28} = 11.3$ , $P = 0.002$																																																																																			
		Active	-1.86 $\pm$ 0.24	-2.24 $\pm$ 0.26*#				N33	Cp1	Sham	-0.59 $\pm$ 0.21	-0.11 $\pm$ 0.17*	$F_{1,28} = 10.3$ , $P = 0.003$	$F_{1,28} = 0.29$ , $P = 0.592$	$F_{1,28} = 1.00$ , $P = 0.326$	Active	-0.60 $\pm$ 0.20	-0.35 $\pm$ 0.23*	P45	Cp1	Sham	1.35 $\pm$ 0.16	1.59 $\pm$ 0.22*	$F_{1,28} = 9.8$ , $P = 0.004$	$F_{1,28} = 1.2$ , $P = 0.276$	$F_{1,28} = 2.1$ , $P = 0.161$	Active	1.45 $\pm$ 0.26	2.10 $\pm$ 0.30*	N60	Fc1	Sham	-1.44 $\pm$ 0.75	-1.27 $\pm$ 0.24	$F_{1,28} = 1.57$ , $P = 0.219$	$F_{1,28} = 0.72$ , $P = 0.403$	$F_{1,28} = 0.00$ , $P = 0.989$	Active	-1.70 $\pm$ 0.25	-1.56 $\pm$ 0.33																																																		
N33	Cp1	Sham	-0.59 $\pm$ 0.21	-0.11 $\pm$ 0.17*	$F_{1,28} = 10.3$ , $P = 0.003$	$F_{1,28} = 0.29$ , $P = 0.592$	$F_{1,28} = 1.00$ , $P = 0.326$																																																																																			
		Active	-0.60 $\pm$ 0.20	-0.35 $\pm$ 0.23*				P45	Cp1	Sham	1.35 $\pm$ 0.16	1.59 $\pm$ 0.22*	$F_{1,28} = 9.8$ , $P = 0.004$	$F_{1,28} = 1.2$ , $P = 0.276$	$F_{1,28} = 2.1$ , $P = 0.161$	Active	1.45 $\pm$ 0.26	2.10 $\pm$ 0.30*	N60	Fc1	Sham	-1.44 $\pm$ 0.75	-1.27 $\pm$ 0.24	$F_{1,28} = 1.57$ , $P = 0.219$	$F_{1,28} = 0.72$ , $P = 0.403$	$F_{1,28} = 0.00$ , $P = 0.989$	Active	-1.70 $\pm$ 0.25	-1.56 $\pm$ 0.33																																																													
P45	Cp1	Sham	1.35 $\pm$ 0.16	1.59 $\pm$ 0.22*	$F_{1,28} = 9.8$ , $P = 0.004$	$F_{1,28} = 1.2$ , $P = 0.276$	$F_{1,28} = 2.1$ , $P = 0.161$																																																																																			
		Active	1.45 $\pm$ 0.26	2.10 $\pm$ 0.30*				N60	Fc1	Sham	-1.44 $\pm$ 0.75	-1.27 $\pm$ 0.24	$F_{1,28} = 1.57$ , $P = 0.219$	$F_{1,28} = 0.72$ , $P = 0.403$	$F_{1,28} = 0.00$ , $P = 0.989$	Active	-1.70 $\pm$ 0.25	-1.56 $\pm$ 0.33																																																																								
N60	Fc1	Sham	-1.44 $\pm$ 0.75	-1.27 $\pm$ 0.24	$F_{1,28} = 1.57$ , $P = 0.219$	$F_{1,28} = 0.72$ , $P = 0.403$	$F_{1,28} = 0.00$ , $P = 0.989$																																																																																			
		Active	-1.70 $\pm$ 0.25	-1.56 $\pm$ 0.33																																																																																						

and disability in hand function (PRTEE:  $\sim$ 20 (Bergin et al., 2015; Schabrun et al., 2016)), and hyperalgesia (PPT:  $\sim$ 100 kPa reduction (Schabrun et al., 2016)). In contrast, the active rTMS group showed lower levels of muscle soreness, disability in hand function and muscle hyperalgesia, supporting the notion that activation of the left DLPFC is a possible target for pain modulation (Borckardt et al., 2014; Mylius et al., 2012; Taylor et al., 2013). Although the mechanisms involved in this analgesic effect are still debated, possible mechanisms of left DLPFC rTMS analgesia could include activation of the descending modulatory endogenous opioidergic system (Taylor et al., 2013), or the involvement of other mechanisms, such as cognitive behavior or mood state, mediated by glutamatergic, dopaminergic and serotonergic systems (Cho and Strafella, 2009; Ciampi De Andrade et al., 2014; Sibon et al., 2007).

#### 4.2. Effects of sustained muscle soreness and rTMS over left DLPFC on somatosensory cortical excitability

In the current study, the sham group showed a pain-related decrease of the frontal N30 peak amplitude. The exact origin and the physiology of frontal N30 potential remain still arduous and controversial. According to the unifying model, SEPs reflect the activation of a single common generator situated in the parietal lobe (Allison et al., 1989), suggesting that the frontal N30 is the mirror image of the parietal P25-27 component. However, this model has been challenged by evidence also demonstrating an independent frontal generator (Mauguière et al., 1983).

Classically, preparation, execution, observation and imagination of a movement ipsilateral to nerve stimulation have been shown to decrease frontal N30 SEPs (Böcker et al., 1993; Cebolla et al., 2009; Cheron and Borenstein, 1987; Rossi et al., 2002) while an increase of frontal N30 SEPs have been observed during execution of repetitive movements contralateral to nerve stimulation (Legon et al., 2008, 2010; Brown and Staines, 2015), suggesting that frontal N30 SEP is strongly influenced by motor planning or motor execution. Therefore, the frontal N30 SEP has been related to the functionality of several circuits of a complex inter-hemispheric cortico/subcortical network linking basal ganglia, thalamus, pre-frontal, supplementary and pre-motor areas (Barba et al., 2005; Cebolla et al., 2014; Kaňovský et al., 2003; Mauguière et al., 1983). Based on this, the results of this study suggest that muscle soreness induced by NGF altered the activity of some circuits of prefrontal-basal ganglia pathways and may interfere with some aspects of motor planning or motor execution. Importantly, an increase of the centro-parietal P25 potential ( $\sim$ 0.35  $\mu$ V) was also found at Day-5. Consequently, the increase

of the centro-parietal P25 may also lead to a decrease of the frontal N25 (not detected in our data since it is hidden by the N30 SEP potential), possibly due to a shift of the tangential source generating both responses (N25/P25). Therefore, considering this parietal SEP component, the activity of the post-rolandic area may be altered by muscle soreness induced by NGF.

In contrast to the sham group, high frequency rTMS over the left DLPFC was able to increase the frontal N30 SEP, potentially via greater activity of some circuits of basal-ganglia-thalamocortical pathways. Previous studies have shown that different inhibitory and facilitatory rTMS paradigms over different prefrontal and premotor areas are able to regulate frontal N30 SEP (Brown and Staines, 2016; Hosono et al., 2008; Urushihara et al., 2006), indicating that rTMS over the frontal cortex temporarily modifies some circuits of prefrontal-basal ganglia pathways.

In addition, current results show that the mean difference changes across days in the frontal N30 SEP were associated with the changes in the muscle soreness and muscle hyperalgesia, suggesting that increase of this neural frontal network can be connected with pain relief effect. Data supporting a role for the prefrontal-basal ganglia function in pain and analgesia processing have been derived from numerous preclinical studies and clinical studies (Borsook et al., 2010; Chudler and Dong, 1995), suggesting an interconnection between the functionality of the prefrontal-basal ganglia network and pain perception. For instance, in the clinical domain, two disease patterns suggest a key role of the basal ganglia in pain: Parkinson disease and Complex Regional Pain Syndrome (CRPS). Both of them involve impairment of dopaminergic neurons in the basal ganglia, resulting in movement disorders and affected subjects frequently report chronic pain (Borsook et al., 2010).

In contrast with the frontal N30 peak amplitude, a similar increase of the central-parietal N33-P45 amplitude was found in both groups. When muscle soreness over several days was induced by intramuscular injections of NGF and eccentric exercise inducing delayed-onset muscle soreness was used subsequently, increased central-parietal N33-P45 amplitude was previously demonstrated (De Martino et al., 2018). These centro-parietal cortical changes to low-threshold afferent discharge have been interpreted as an adaptation of cortical processing of somatosensory afferent information since no participants reported ongoing muscle pain at rest during the electrical stimulation (De Martino et al., 2018). However, it is important to notice that P45 amplitude is also affected by attention (Garcia-Larrea et al., 1991) and it cannot be excluded that the changes of P45 amplitude can be explained by changes in the subject's attention to the affected territory.

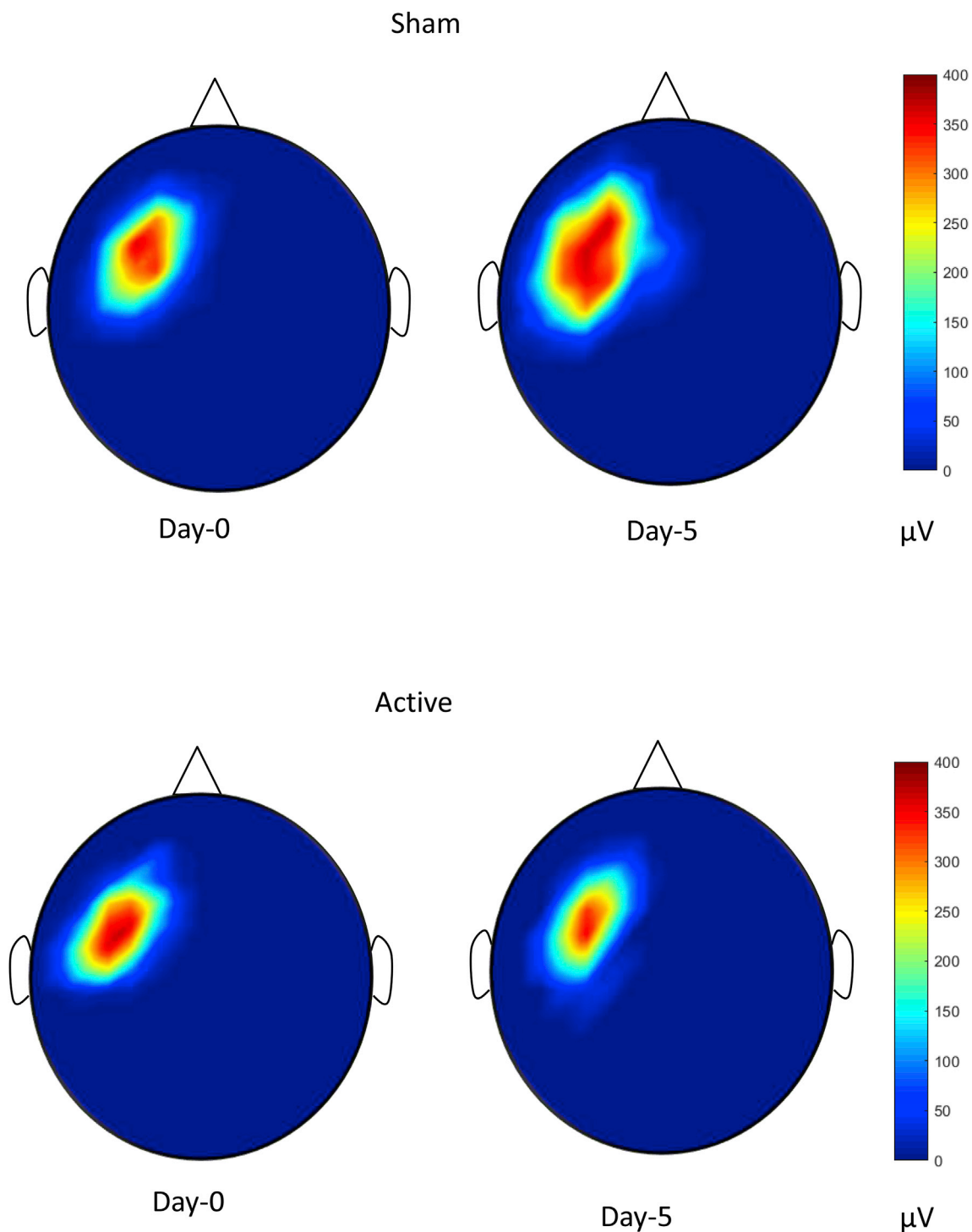


**Fig. 3.** Averaged ( $N = 15$ ) peak-to-peak MEP amplitudes of the right extensor carpi radialis brevis muscle interpolated across stimulation sites at Day-0 and Day-5 in the group receiving sham ( $N = 15$ , top) and active ( $N = 15$ , lower) rTMS applied daily at Day-0 to Day-4. The color scale represents amplitude (from 0 to 400  $\mu\text{V}$ ).

#### 4.3. Effects of sustained muscle soreness and rTMS over left DLPFC on corticomotor excitability

Inducing muscle soreness and hyperalgesia across several days by intramuscular injection of nerve growth factor facilitated motor map volume for up to 2 weeks which reverted when the pain and disability disappeared (De Martino et al., 2018; Schabrun et al., 2016). The sham group in the present study showed a similar increase of motor map volume at Day-5. In contrast, when daily high frequency rTMS stimulations were applied on the DLPFC, depressed motor map volume was detected.

Because of the methodology selected for this study, it is not possible to determine the specific level of the changes in the excitability along the motor pathway in the sham and active group. Indeed, the amplitude of the MEP reflects the motor cortical and spinal motoneuron excitability. In addition, an important issue of the mechanism of action of rTMS is that the effects are not localized only to the stimulated region but spread over distant interconnected cortical, subcortical, and spinal structures (Kobayashi and Pascual-Leone, 2003; Vink et al., 2018), reaching also subcortical and spinal structures that may be involved in the mechanism of pain neuroplasticity. A possible explanation of the contraction of the

**Table 3**

Mean ( $\pm$ SEM, N = 15 per group) parameters related with motor-evoked potentials (MEPs). F-values and P-values are from the mixed model repeated-measures ANOVA. The center of gravity (CoG) position (latitude and longitude) defines the MEP amplitude-weighted center of the map. rMT: resting motor threshold. Significant post-hoc tests from Day-0 within the group (\*,  $P < 0.05$ ) and between groups within the day (#,  $P < 0.05$ ).

	Group	Day-0	Day-5	Mixed model repeated-measures ANOVA		
				Day	Group	Day by Group
rMT (%)	Sham	42.9 $\pm$ 2.6	41.7 $\pm$ 2.2	$F_{1,28} = 0.09$ , $P = 0.766$	$F_{1,28} = 0.11$ , $P = 0.738$	$F_{1,28} = 6.54$ , $P = 0.016$
	Active	42.9 $\pm$ 2.3	43.9 $\pm$ 2.5			
MEP amplitude ( $\mu$ V)	Sham	351.8 $\pm$ 43.6	408.3 $\pm$ 59.6	$F_{1,28} = 0.19$ , $P = 0.663$	$F_{1,28} = 0.38$ , $P = 0.847$	$F_{1,28} = 5.30$ , $P = 0.029$
	Active	434.5 $\pm$ 51.0	351.3 $\pm$ 50.7			
Map volume (mV)	Sham	3025.0 $\pm$ 407.2	3988.7 $\pm$ 447.9*#	$F_{1,28} = 0.05$ , $P = 0.817$	$F_{1,28} = 2.01$ , $P = 0.167$	$F_{1,28} = 35.59$ , $P < 0.001$
	Active	3251.8 $\pm$ 333.3	2360.8 $\pm$ 232.1*#			
Map area (active sites)	Sham	15.7 $\pm$ 1.1	20.3 $\pm$ 1.3*#	$F_{1,28} = 9.51$ , $P = 0.005$	$F_{1,28} = 5.18$ , $P = 0.031$	$F_{1,28} = 26.01$ , $P < 0.001$
	Active	15.2 $\pm$ 1.2	14.1 $\pm$ 0.9#			
CoG latitude (cm)	Sham	5.8 $\pm$ 0.2	5.9 $\pm$ 0.1	$F_{1,28} = 0.02$ , $P = 0.890$	$F_{1,28} = 0.75$ , $P = 0.391$	$F_{1,28} = 3.69$ , $P = 0.065$
	Active	5.7 $\pm$ 0.1	5.6 $\pm$ 0.1			
CoG longitude (cm)	Sham	1.8 $\pm$ 0.2	1.8 $\pm$ 0.2	$F_{1,28} = 1.20$ , $P = 0.282$	$F_{1,28} = 0.04$ , $P = 0.839$	$F_{1,28} = 0.12$ , $P = 0.725$
	Active	1.8 $\pm$ 0.1	1.9 $\pm$ 0.1			

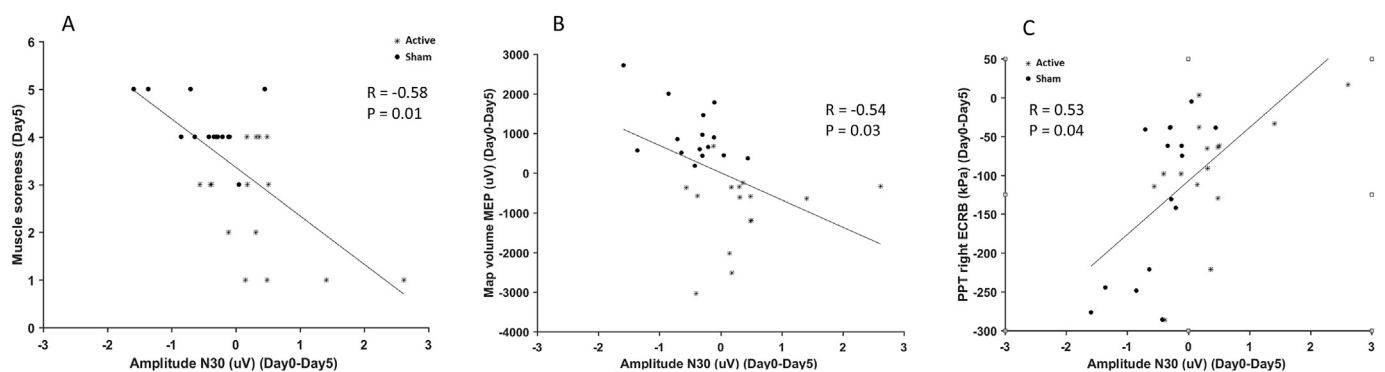


**Fig. 4.** Correlations between changes in Likert scale scores of muscle soreness, pressure pain thresholds (PPTs) on the ECRB muscle, Motor evoked potential (MEP) map volume, and sensory evoked potential (SEP) N30 amplitude (F1) (data expressed as the difference relative to Day-0). The analyses and plots include all 30 subjects.

motor map excitability is that the activation of left DLPFC by rTMS during pain has an analgesic effect and, consequently, a modulatory effect on the expanded motor map. An alternative explanation is that the multiple acute pain sensations that the participants experienced during active rTMS. In fact, the inhibition of MEPs has been described during and after acute pain (Burns et al., 2016), even though 24 h interval divided the last rTMS stimulation and the data collection at Day-5. In addition, the MEPs were collected from ECRB muscle while pain induced by rTMS was localized around the area of stimulation, making unlikely a widespread motor cortex inhibition induced by multiple acute pain sensations.

Importantly, the changes found in the rMT at Day-5 cannot explain the changes in the motor map volume in the two groups because the rMT increased in the active group whereas it decreased in the sham group. Consequently, the intensity of the stimulator output used to motor map at Day-5 was higher in the active group and lower in the sham group compared with Day-0.

The effect of high frequency rTMS on DLPFC on the corticomotor has been previously studied (Fierro et al., 2010; Grunhaus et al., 2003; Rollnik et al., 2000). Rollnik et al. (2000), reported reduced MEPs after applying rTMS on DLPFC in healthy subjects while, Fierro et al. (2010) and Grunhaus et al. (2003) did not find any inhibitory effect 10 and 30 min after rTMS on DLPFC, suggesting short-lasting inhibitory effects on the MEPs after a single short-lasting session. Based on animal and human studies, when multiple sessions of rTMS are delivered cumulative neuroplastic and therapeutic effects have been reported (Abraham et al., 2002; George et al., 2010a,b; Goldsworthy et al., 2012), suggesting long-lasting neuroplastic effect induced by multiple daily sessions of rTMS.

So far, only one study investigated combined cortical effects of rTMS on DLPFC on the MEPs during short-term experimental pain, demonstrating that a single session of rTMS on DLPFC was able to produce analgesic effects and reverse cortical neuroplastic pain-related changes induced by the application of capsaicin cream (Fierro et al., 2010). Such findings support the notion that the activation of left DLPFC by rTMS during short-lasting pain has an analgesic effect and modulatory effects on the corticomotor excitability (Fierro et al., 2010). In addition, the present study showed that the changes across days in the SEP N30 amplitude were associated with the changes in the motor map volume, suggesting a possible functional connection between the frontal neural network and motor cortex excitability during muscle soreness induced by NGF.

#### 4.4. Limitations

There were some limitations to the study. A first limitation of this study was the single blind. While participants did not know the type of stimulation they received, the experimenter involved in data collection was not blinded. A second limitation of this study was the visual inspection of hand movements to determine rMT to set the intensity of rTMS. Although this method is one of the most commonly used in clinical settings (George et al., 2010a,b), this approach provides higher values for this parameter compared with rMT based on MEPs. A third limitation is that the participants were not asked to guess whether they had received real TMS or sham TMS. However, all our participants were naïve to TMS and rTMS prior to enrolment. Finally, the F3beam approach has been used in this project to locate the coil to stimulate the left DLPFC since MRI-based neuronavigation was unavailable.

## 5. Conclusions

Multiple sessions of high frequency rTMS over left DLPFC reduced motor map volume normally increased by prolonged muscle pain and increased frontal N30 SEPs, which is thought to be linked to prefrontal-basal ganglia function. In addition, these sensorimotor cortical excitability changes were associated with pain perception in the pain model. These results suggest that multiple applications of high frequency rTMS over DLPFC are able to modulate the sensorimotor cortical excitability (motor and sensory evoked potentials) induced by sustained muscle soreness, probably by the prefrontal-basal ganglia network. Future experiments are needed to test more directly this possible mechanism.

## Acknowledgments

Center for Neuroplasticity and Pain (CNAP) is supported by the Danish National Research Foundation (DNRF121). SMS receives salary support from the National Health and Medical Research Council of Australia (NHMRC, 1105040). The authors have no conflict of interest to report.

## Appendix A. Supplementary data

Supplementary data to this article can be found online at <https://doi.org/10.1016/j.neuroimage.2018.10.076>.

## References

- Abraham, W.C., Logan, B., Greenwood, J.M., Dragunow, M., 2002. Induction and experience-dependent consolidation of stable long-term potentiation lasting months in the hippocampus. *J. Neurosci.* 22 (21), 9626–9634. <http://doi.org/10.1523/JNEUROSCI.3644-07.2007>.
- Alexander, G., 1986. Parallel organization of functionally segregated circuits linking basal ganglia and cortex. *Annu. Rev. Neurosci.* 9 (1), 357–381. <http://doi.org/10.1146/annurev.neuro.9.1.357>.
- Allison, T., McCarthy, G., Wood, C.C., Darcey, T.M., Spencer, D.D., Williamson, P.D., Spencer, D.D., 1989. Human cortical potentials evoked by stimulation of the median nerve. I. Cytoarchitectonic areas generating short-latency activity. *J. Neurophysiol.* 62 (3), 711–722.
- Aron, A.R., Durston, S., Eagle, D.M., Logan, G.D., Stinear, C.M., Stuphorn, V., 2007. Converging evidence for a fronto-basal-ganglia network for inhibitory control of action and cognition. *J. Neurosci.* 27 (44), 11860–11864. <http://doi.org/10.1523/JNEUROSCI.3644-07.2007>.
- Barba, C., Valeriani, M., Colicchio, G., Mauguère, F., 2005. Short and middle-latency Median Nerve (MN) SEPs recorded by depth electrodes in human pre-SMA and SMA-proper. *Clin. Neurophysiol.* 116 (11), 2664–2674. <http://doi.org/10.1016/j.clinph.2005.07.022>.
- Beam, W., Borckardt, J.J., Scott, T., Reeves, M.D., Mark, S., George, M.D., 2009. An efficient and accurate new method for locating the F3 position for prefrontal TMS applications William. *Brain Stimul.* 1 (2), 50–54. <http://doi.org/10.1097/MCA.0000000000000178>.
- Bergin, M.J.G., Hirata, R., Mista, C., Christensen, S.W., Tucker, K., Vicenzino, B., et al., 2015. Movement evoked pain and mechanical hyperalgesia after intramuscular injection of nerve growth factor: a model of sustained elbow pain. *Pain Med.* 16 (11), 2180–2191. <http://doi.org/10.1111/pme.12824>.
- Borckardt, J.J., Nahas, Z.H., Teal, J., Lisanby, S.H., McDonald, M., Avery, D., et al., 2013. The painfulness of active, but not sham, transcranial magnetic stimulation decreases rapidly over time: results from the double-blind phase of the OPT-TMS trial. *Brain Stimul.* 6 (6), 1–8. <http://doi.org/10.1016/j.brs.2013.04.009>.
- Borckardt, J.J., Reeves, S.T., Kotlowski, P., Abernathy, J.H., Field, L.C., Dong, L., et al., 2014. Fast left prefrontal rTMS reduces post-gastric bypass surgery pain: findings from a large-scale, double-blind, sham-controlled clinical trial. *Brain Stimul.* 7 (1), 42–48. <http://doi.org/10.1016/j.brs.2013.07.007>.
- Borckardt, J.J., Reeves, S., Weinstein, M., Smith, A., Shelley, N., Kozel, F.A., et al., 2008. Significant analgesic effects of one session of postoperative left prefrontal cortex repetitive transcranial magnetic stimulation: a replication study. *Brain Stimul.* 1 (2), 122–127. <http://doi.org/10.1016/j.brs.2008.04.002>. Significant.
- Borckardt, J.J., Smith, A.R., Hutcheson, K., Johnson, K., Nahas, Z., Anderson, B., et al., 2006. Reducing pain and unpleasantness during repetitive transcranial magnetic stimulation. *J. ECT* 22 (4), 259–264. <http://doi.org/10.1097/01.yct.0000244248.40662.9a>.
- Borsook, D., Upadhyay, J., Chudler, E.H., Becerra, L., 2010. A key role of the basal ganglia in pain and analgesia—insights gained through human functional imaging. *Mol. Pain* 6, 27. <http://doi.org/10.1186/1744-8069-6-27>.
- Brown, M.J.N., Staines, W.R., 2016. Somatosensory input to non-primary motor areas is enhanced during preparation of cued contralateral finger sequence movements. *Behav. Brain Res.* 286, 166–174. <http://doi.org/10.1016/j.bbr.2015.02.052>.
- Brown, M.J.N., Staines, W.R., 2016. Differential effects of continuous theta burst stimulation over left premotor cortex and right prefrontal cortex on modulating upper limb somatosensory input. *Neuroimage* 127, 97–109. <http://doi.org/10.1016/j.neuroimage.2015.11.051>.
- Burns, E., Chipchase, L.S., Schabrun, S.M., 2016. Primary sensory and motor cortex function in response to acute muscle pain: a systematic review and meta-analysis. *Eur. J. Pain* 20 (8), 1203–1213. <http://doi.org/10.1002/ejp.859>.
- Böcker, K.B.E., Forget, R., Brunia, C.H.M., 1993. The modulation of somatosensory evoked potentials during the foreperiod of a forewarned reaction time task. *Electroencephalogr. Clin. Neurophysiol. Evoked Potentials* 88 (2), 105–117. [http://doi.org/10.1016/0168-5597\(93\)90061-S](http://doi.org/10.1016/0168-5597(93)90061-S).
- Cebolla, A.M., De Saedeleer, C., Bengoetxea, A., Leurs, F., Balestra, C., D'Alcantara, P., et al., 2009. Movement gating of beta/gamma oscillations involved in the N30 somatosensory evoked potential. *Hum. Brain Mapp.* 30 (5), 1568–1579. <http://doi.org/10.1002/hbm.20624>.
- Cebolla, A.M., Palmero-Soler, E., Dan, B., Cheron, G., 2011. Frontal phasic and oscillatory generators of the N30 somatosensory evoked potential. *Neuroimage* 54 (2), 1297–1306. <http://doi.org/10.1016/j.neuroimage.2010.08.060>.
- Cebolla, A.M., Palmero-Soler, E., Dan, B., Cheron, G., 2014. Modulation of the N30 generators of the somatosensory evoked potentials by the mirror neuron system. *Neuroimage* 95, 48–60. <http://doi.org/10.1016/j.neuroimage.2014.03.039>.
- Chang, W.J., O'Connell, N.E., Beckenkamp, P.R., Alhassani, G., Liston, M.B., Schabrun, S.M., 2018. Altered primary motor cortex structure, organization, and function in chronic pain: a systematic review and meta-analysis. *J. Pain* 19 (4), 341–359. <http://doi.org/10.1016/j.jpain.2017.10.007>.
- Chen, R., Classen, J., Gerloff, C., Celnik, P., Wassermann, E.M., Hallett, M., Cohen, L.G., 1997. Depression of motor cortex excitability by low-frequency transcranial magnetic stimulation. *Neurology* 48 (5), 1398–1403. <http://doi.org/10.1212/WNL.48.5.1398>.
- Cheron, G., Borenstein, S., 1987. Specific gating of the early somatosensory evoked potentials during active movement. In: *Electroencephalography and Clinical Neurophysiology*, 67, pp. 537–548.
- Cho, S.S., Strafella, A.P., 2009. rTMS of the left dorsolateral prefrontal cortex modulates dopamine release in the ipsilateral anterior cingulate cortex and orbitofrontal cortex. *PLoS One* 4 (8), 2–9. <http://doi.org/10.1371/journal.pone.0006725>.
- Chudler, E.H., Dong, W.K., 1995. The role of the basal ganglia in nociception and pain. *Pain* 60 (1), 3–38. [http://doi.org/10.1016/0304-3959\(94\)00172-B](http://doi.org/10.1016/0304-3959(94)00172-B).
- Ciampi De Andrade, D., Mhalla, A., Adam, F., Teixeira, M.J., Bouhassira, D., 2014. Repetitive transcranial magnetic stimulation induced analgesia depends on N-methyl-D-aspartate glutamate receptors. *Pain* 155 (3), 598–605. <http://doi.org/10.1016/j.pain.2013.12.022>.
- De Martino, E., Zandalasini, M., Schabrun, S., Petrini, L., Graven-Nielsen, T., 2018. Experimental muscle hyperalgesia modulates sensorimotor cortical excitability, which is partially altered by unaccustomed exercise. *Pain* (1), 1. <http://doi.org/10.1097/j.pain.0000000000001351>.
- Desmedt, J.E., Cheron, G., 1980. Central somatosensory conduction in man: neural generators and interpeak latencies of the far-field components recorded from neck and right or left scalp and earlobes. *Electroencephalogr. Clin. Neurophysiol.* 50 (5–6), 382–403. [http://doi.org/10.1016/0013-4694\(80\)90006-1](http://doi.org/10.1016/0013-4694(80)90006-1).
- Fierro, B., De Tommaso, M., Giglia, F., Giglia, G., Palermo, A., Brighina, F., 2010. Repetitive transcranial magnetic stimulation (rTMS) of the dorsolateral prefrontal cortex (DLPFC) during capsaicin-induced pain: modulatory effects on motor cortex excitability. *Exp. Brain Res.* 203 (1), 31–38. <http://doi.org/10.1007/s00221-010-2206-6>.
- Flor, H., Braun, C., Elbert, T., Birbaumer, N., 1997. Extensive reorganization of primary somatosensory cortex in chronic back pain patients. *Neurosci. Lett.* 224 (1), 5–8. [http://doi.org/10.1016/S0304-3940\(97\)13441-3](http://doi.org/10.1016/S0304-3940(97)13441-3).
- Freund, W., Weber, F., Stuber, G., Schmitz, B., Wunderlich, A.P., 2009. Perception and suppression of thermally induced pain: a fMRI study. *Somatosens. Mot. Res.* 26 (1), 1–10. <http://doi.org/10.1080/08990220902738243>.
- García-Larrea, L., Bastuji, H., Mauguère, F., 1991. Mapping study of somatosensory evoked potentials during selective spatial attention. *Electroencephalogr. Clin. Neurophysiol.* 80 (3), 201–214.
- George, M.S., Lisanby, S.H., Avery, D., McDonald, W.M., Durkalski, V., Pavlicova, M., et al., 2010a. Daily left prefrontal transcranial magnetic stimulation therapy for major depressive disorder. *Arch. Gen. Psychiatr.* 67 (5), 507. <http://doi.org/10.1001/archgenpsychiatry.2010.46>.
- George, M.S., Lisanby, S.H., Avery, D., McDonald, W.M., Durkalski, V., Pavlicova, M., et al., 2010b. Daily left prefrontal transcranial magnetic stimulation therapy for major depressive disorder. *Arch. Gen. Psychiatr.* 67 (5), 507–516. <http://doi.org/10.1001/archgenpsychiatry.2010.46>.
- Glasser, M.F., Coalson, T.S., Robinson, E.C., Hacker, C.D., Harwell, J., Yacoub, E., et al., 2016. A multi-modal parcellation of human cerebral cortex. *Nature* 536 (7615), 171–178. <http://doi.org/10.1038/nature18933>.
- Goldsworthy, M.R., Pitcher, J.B., Ridding, M.C., 2012. The application of spaced theta burst protocols induces long-lasting neuroplastic changes in the human motor cortex. *Eur. J. Neurosci.* 35 (1), 125–134. <http://doi.org/10.1111/j.1460-9568.2011.07924.x>.
- Grunhaus, L., Polak, D., Amiaz, R., Dannon, P.N., 2003. Motor-evoked potential amplitudes elicited by transcranial magnetic stimulation do not differentiate between patients and normal controls. *Int. J. Neuropsychopharmacol.* 6 (April), 371–378. <http://doi.org/10.1017/S1461145703003705>.
- Hosono, Y., Urushihara, R., Harada, M., Morita, N., Murase, N., Kunikane, Y., et al., 2008. Comparison of monophasic versus biphasic stimulation in rTMS over premotor cortex: SEP and SPECT studies. *Clin. Neurophysiol.* 119 (11), 2538–2545. <http://doi.org/10.1016/j.clinph.2008.07.279>.
- Kaňovský, P., Bares, M., Rektor, I., 2003. The selective gating of the N30 cortical component of the somatosensory evoked potentials of median nerve is different in the

- mesial and dorsolateral frontal cortex: evidence from intracerebral recordings. *Clin. Neurophysiol.* 114 (6), 981–991. [http://doi.org/10.1016/S1388-2457\(03\)00068-3](http://doi.org/10.1016/S1388-2457(03)00068-3).
- Kobayashi, M., Pascual-Leone, A., 2003. Transcranial magnetic stimulation in neurology. *Lancet Neurol.* 2 (3), 145–156. [http://doi.org/10.1016/S1474-4422\(03\)00321-1](http://doi.org/10.1016/S1474-4422(03)00321-1).
- Kuner, R., Flor, H., 2016. Structural plasticity and reorganisation in chronic pain. *Nat. Rev. Neurosci.* 18 (1), 20–30. <http://doi.org/10.1038/nrn.2016.162>.
- Le Pera, D., Graven-Nielsen, T., Valeriani, M., Oliviero, A., Di Lazzaro, V., Tonali, P.A., Arendt-Nielsen, L., 2001. Inhibition of motor system excitability at cortical and spinal level by tonic muscle pain. *Clin. Neurophysiol.* 112 (9), 1633–1641. [http://doi.org/10.1016/S1388-2457\(01\)00631-9](http://doi.org/10.1016/S1388-2457(01)00631-9).
- Lefaucheur, J.P., André-Obadia, N., Antal, A., Ayache, S.S., Baeken, C., Benninger, D.H., et al., 2014. Evidence-based guidelines on the therapeutic use of repetitive transcranial magnetic stimulation (rTMS). *Clin. Neurophysiol.* 125 (11), 2150–2206. <http://doi.org/10.1016/j.clinph.2014.05.021>.
- Legon, W., Dionne, J.K., Meehan, S.K., Staines, W.R., 2010. Non-dominant hand movement facilitates the frontal N30 somatosensory evoked potential. *BMC Neurosci.* 11. <http://doi.org/10.1186/1471-2202-11-112>.
- Legon, W., Meehan, S.K., Staines, W.R., 2008. The relationship between frontal somatosensory-evoked potentials and motor planning. *Neuroreport* 19 (1), 87–91. <http://doi.org/10.1097/WNR.0b013e3282f36f5f>.
- MacDermid, J., 2005. Update: the patient-rated forearm evaluation questionnaire is now the patient-rated tenic elbow evaluation. *J. Hand Ther.* 18 (4), 407–410. <http://doi.org/10.1197/j.jht.2005.07.002>.
- Mauguière, F., Desmedt, J.E., Courjon, J., 1983. Astereognosis and dissociated loss of frontal or parietal components of somatosensory evoked potentials in hemispheric lesions: detailed correlations with clinical signs and computerized tomographic scanning. *Brain* 106 (2), 271–311. <http://doi.org/10.1093/brain/106.2.271>.
- Middleton, F.A., 2002. Basal-ganglia “projections” to the prefrontal cortex of the primate. *Cerebr. Cortex* 12 (9), 926–935. <http://doi.org/10.1093/cercor/12.9.926>.
- Mir-Moghtadaei, A., Caballero, R., Fried, P., Fox, M.D., Lee, K., Giacobbe, P., et al., 2016. Concordance between BeamF3 and MRI-neuronavigated target sites for repetitive transcranial magnetic stimulation of the left dorsolateral prefrontal cortex arsalan. *Brain Stimul.* 1848 (5), 3047–3054. <http://doi.org/10.1016/j.bbsmem.2015.02.010>.
- Cationic.
- Mista, C.A., Bergin, M.J.G., Hirata, R.P., Christensen, S.W., Tucker, K., Hodges, P., Graven-Nielsen, T., 2016. Effects of prolonged and acute muscle pain on the force control strategy during isometric contractions. *J. Pain* 17 (10), 1116–1125. <http://doi.org/10.1016/j.jpain.2016.06.013>.
- Mylius, V., Borckardt, J.J., Lefaucheur, J.-P., 2012. Noninvasive Cortical Modulation of Experimental Pain, pp. 1350–1363. TL - 153. *Pain*, 153 VN-7. <http://doi.org/10.1016/j.pain.2012.04.009>.
- Oostenveld, R., Praamstra, P., 2001. The five percent electrode system for high-resolution EEG and ERP measurements. *Clin. Neurophysiol.* 112 (4), 713–719. [http://doi.org/10.1016/S1388-2457\(00\)00527-7](http://doi.org/10.1016/S1388-2457(00)00527-7).
- Pascual-Leone, A., Grafman, J., Hallett, M., 1994a. Modulation of cortical motor output maps during development. *Science* 263, 1287–1289.
- Pascual-Leone, A., Valls-Sole, J., Wassermann, E.M., Hallett, M., 1994b. Responses to rapid-rate transcranial magnetic stimulation of the human motor cortex. *Brain: J. Neurol.* 117, 847–858. Retrieved from. [http://www.Users/kaminkim/Library/Application Support/Zotero/Profiles/5z77uulf.default/zotero/storage/NQKX3VBI/\\_DanaInfo=ucdavis.worldcat.html](http://www.Users/kaminkim/Library/Application%20Support/Zotero/Profiles/5z77uulf.default/zotero/storage/NQKX3VBI/_DanaInfo=ucdavis.worldcat.html).
- Rollnik, J.D., Schubert, M., Dengler, R., 2000. Subthreshold prefrontal repetitive transcranial magnetic stimulation reduces motor cortex excitability. *Muscle Nerve* 23 (1), 112–114. [http://doi.org/10.1002/\(SICI\)1097-4598\(200001\)23:1%0c112::AID-MUS15%0e3.0.CO;2-B](http://doi.org/10.1002/(SICI)1097-4598(200001)23:1%0c112::AID-MUS15%0e3.0.CO;2-B).
- Rossi, S., Della Volpe, R., Ginanneschi, F., Olivelli, M., Bartalini, S., Spidalieri, R., Rossi, A., 2003. Early somatosensory processing during tonic muscle pain in humans: relation to loss of proprioception and motor “defensive” strategies. *Clin. Neurophysiol.* 114 (7), 1351–1358. [http://doi.org/10.1016/S1388-2457\(03\)00073-7](http://doi.org/10.1016/S1388-2457(03)00073-7).
- Rossi, S., Hallett, M., Rossini, P.M., Pascual-Leone, A., 2012. Safety, ethical considerations, and application guidelines for the use of transcranial magnetic stimulation in clinical practice and research. *Clin. Neurophysiol.* 120 (12), 323–330. <http://doi.org/10.1016/j.clinph.2009.08.016.Rossi>.
- Rossi, S., Tecchio, F., Pasqualetti, P., Olivelli, M., Pizzella, V., Romani, G.L., et al., 2002. Somatosensory processing during movement observation in humans. *Clin. Neurophysiol.* 113 (1), 16–24. [http://doi.org/10.1016/S1388-2457\(01\)00725-8](http://doi.org/10.1016/S1388-2457(01)00725-8).
- Rossini, P.M., Burke, D., Chen, R., Cohen, L.G., Daskalakis, Z., Di Iorio, R., et al., 2015. Non-invasive electrical and magnetic stimulation of the brain, spinal cord, roots and peripheral nerves: basic principles and procedures for routine clinical and research application: an updated report from an I.F.C.N. Committee. *Clin. Neurophysiol.* 126 (6), 1071–1107. <http://doi.org/10.1016/j.clinph.2015.02.001>.
- Schabrun, S.M., Christensen, S.W., Mrachacz-Kersting, N., Graven-Nielsen, T., 2016. Motor cortex reorganization and impaired function in the transition to sustained muscle pain. *Cerebr. Cortex* 26 (5), 1878–1890. <http://doi.org/10.1093/cercor/bhu319>.
- Schabrun, S.M., Ridding, M.C., 2007. The influence of correlated afferent input on motor cortical representations in humans. *Exp. Brain Res.* 183 (1), 41–49. <http://doi.org/10.1007/s00221-007-1019-8>.
- Seminowicz, D.A., de Martino, E., Schabrun, S.M., Graven-Nielsen, T., 2018. Left DLPFC Somatosensory Processing during the Development of Long-term Muscle Pain. *Pain*, 1. <http://doi.org/10.1097/j.pain.0000000000001350>.
- Seminowicz, D.A., Moayed, M., 2017. The dorsolateral prefrontal cortex in acute and chronic pain. *J. Pain* 18 (9), 1027–1035. <http://doi.org/10.1016/j.jpain.2017.03.008>.
- Sibon, I., Strafella, A.P., Gravel, P., Ko, J.H., Booi, L., Soucy, J.P., et al., 2007. Acute prefrontal cortex TMS in healthy volunteers: effects on brain11C-αMtrp trapping. *Neuroimage* 34 (4), 1658–1664. <http://doi.org/10.1016/j.neuroimage.2006.08.059>.
- Taylor, J.J., Borckardt, J.J., Canterberry, M., Li, X., Hanlon, C.A., Brown, T.R., George, M.S., 2013. Naloxone-reversible modulation of pain circuitry by left prefrontal RTMS. *Neuropsychopharmacology* 38 (7), 1189–1197. <http://doi.org/10.1038/npp.2013.13>.
- Taylor, J.J., Borckardt, J.J., George, M.S., 2012. Endogenous opioids mediate left dorsolateral prefrontal cortex rTMS-induced analgesia. *Pain* 153 (6), 1219–1225. <http://doi.org/10.1016/j.pain.2012.02.030>.
- Tinazzi, M., Zanette, G., Polo, A., Volpato, D., Manganotti, P., 1997. Transient deafferentation in humans induces rapid modulation of primary sensory cortex not associated with subcortical changes: a somatosensory evoked potential study. *Neurosci. Lett.* 223, 21–24.
- Tsao, H., Galea, M.P., Hodges, P.W., 2008. Reorganization of the motor cortex is associated with postural control deficits in recurrent low back pain. *Brain* 131 (8), 2161–2171. <http://doi.org/10.1093/brain/awn154>.
- Urushihara, R., Murase, N., Rothwell, J.C., Harada, M., Hosono, Y., Asanuma, K., et al., 2006. Effect of repetitive transcranial magnetic stimulation applied over the premotor cortex on somatosensory-evoked potentials and regional cerebral blood flow. *Neuroimage* 31 (2), 699–709. <http://doi.org/10.1016/j.neuroimage.2005.12.027>.
- Uy, J., Ridding, M.C., Miles, T.S., 2002. Stability of Maps of Human Motor Cortex Made with Transcranial Magnetic Stimulation, 14, pp. 293–297 (4).
- Valeriani, M., Le Pera, D., Tonali, P., 2001. Characterizing somatosensory evoked potential sources with dipole models: advantages and limitations. *Muscle Nerve* 24 (3), 325–339. [http://doi.org/10.1002/1097-4598\(200103\)24:3%0c325::AID-MUS1002%0e3.0.CO;2-0](http://doi.org/10.1002/1097-4598(200103)24:3%0c325::AID-MUS1002%0e3.0.CO;2-0).
- Vink, J.J.T., Mandija, S., Petrov, P.I., van den Berg, C.A.T., Sommer, I.E.C., Neggers, S.F.W., 2018. A novel concurrent TMS-fMRI method to reveal propagation patterns of prefrontal magnetic brain stimulation. *Hum. Brain Mapp.* 1–13 (June). <http://doi.org/10.1002/hbm.24307>.
- Wassermann, E.M., McShane, L.M., Hallett, M., Cohen, L.G., 1992 Feb. Noninvasive mapping of muscle representations in human motor cortex. *Electroencephalogr. Clin. Neurophysiol.* 85 (1), 1–8.
- Ziemann, U., Paulus, W., Nitsche, M.A., Pascual-Leone, A., Byblow, W.D., Berardelli, A., et al., 2008. Consensus: motor cortex plasticity protocols. *Brain Stimul.* 1 (3), 164–182. <http://doi.org/10.1016/j.brs.2008.06.006>.